THE ANATOMICAL RECORD 302:2287–2299 (2019)

Bite Force and Masticatory Muscle Architecture Adaptations in the Dietarily Diverse Musteloidea (Carnivora)

ADAM HARTSTONE-ROSE,* ISABELLA HERTZIG, AND EDWIN DICKINSON
Department of Biological Sciences, North Carolina State University, Raleigh, North Carolina

ABSTRACT

Dietary ecology and its relationship with both muscle architecture and bite force potential has been studied in many mammalian (and non-mammalian) taxa. However, despite the diversity of dietary niches that characterizes the superfamily Musteloidea, the masticatory muscle fiber architecture of its members has yet to be investigated anatomically. In this study, we present myological data from the jaw adductors in combination with biomechanical data derived from craniomandibular measurements for 17 species representing all four families (Ailuridae, Mephitidae, Mustelidae, and Procyonidae) of Musteloid. These data are combined to calculate bite force potential at each of three bite points along the dental row. Across our sample as a whole, masticatory muscle mass scaled with isometry or slight positive allometry against both body mass and skull size (measured via a cranial geometric mean). Total jaw adductor physiological cross-sectional area scaled with positive allometry against both body mass and skull size, while weighted fiber length scaled with negative allometry. From a dietary perspective, fiber length is strongly correlated with dietary size such that taxa that exploit larger foods demonstrated myological adaptations toward gape maximization. However, no consistent relationship between bite force potential and dietary mechanical resistance was observed. These trends confirm previous findings observed within the carnivoran family Felidae (as well as within primates), suggesting that the mechanisms by which masticatory anatomy adapts to dietary ecology may be more universally consistent than previously recognized. Anat Rec, 302:2287–2299, 2019. © 2019 American Association for Anatomy

Key words: Carnivora; scaling; PCSA; fiber length; mechanical advantage

Musteloidea is a taxonomic superfamily within the order Carnivora that consists of the families Ailuridae (the red panda), Mephitidae (skunks), Mustelidae (badgers, martens, minks, otters, weasels, and wolverines), and Procyonidae (coatis, kinkajous, raccoons, and ringtails; Wilson and Mittermeier, 2009). These taxa exhibit many morphological similarities (Goswami, 2006) but encompass a wide range of dietary niches: ranging from specialized durophagy and hypercarnivory to generalized omnivory (Larivière and Walton, 1998; Zabala and Zuberogoitia, 2003; Alves-Costa et al., 2004; Gatti et al., 2006; Dalerum et al., 2009; Ferreira et al., 2013). Specifically, musteloid diets include fish and marine invertebrates [e.g., *Lontra canadensis*; Larivière and Walton,

Grant sponsor: National Science Foundation; Grant sponsor: North Carolina Museum of Natural Sciences.

*Correspondence to: Adam Hartstone-Rose, Department of Biological Sciences, North Carolina State University, Raleigh, NC 27695. Fax: 919-515-1761. E-mail: adamhrose@ncsu.edu

Received 17 May 2019; Revised 3 July 2019; Accepted 3 July 2019.

DOI: 10.1002/ar.24233
Published online 10 September 2019 in Wiley Online Library (wileyonlinelibrary.com).

1998), small mammals, insects, fruits, eggs, and even bamboo (*Ailurus fulgens*; Roberts and Gittleman, 1984)]. Within single families and genera, dietary diversification may be high: while the American hog-nosed skunk (*Conepatus leuconotus*) is predominantly insectivorous, the Andean hog-nosed skunk (*Conepatus chinga*) is a dedicated hypercarnivore, exploiting both small vertebrates and invertebrates (Donadio et al., 2004; Montalvo et al., 2008; Dragoo and Sheffield, 2009).

The diets of Musteloidea vary not only in their composition, but also in their relative size and mechanical resistance. Obdurate plant material, such as bamboo, exhibits high degrees of toughness—being capable of absorbing high magnitudes of stress prior to fracture (Hill and Lucas, 1996; Berthaume, 2016). Such foods are difficult to shear, and typically require significant mastication prior to swallowing (Berthaume, 2016). By contrast, the external shells of mollusks are extremely mechanically hard (though much more brittle than wood or bamboo), being capable of resisting high magnitudes of stress (Constantino et al., 2011). Once fractured, however, mollusks expose a soft interior that requires little to no mastication. Some musteloids are capable of cracking large bones (e.g., the wolverine, *Gulo gulo*; Pasitschniak-Arts and Larivière, 1995)—a durophagous diet that is both tough and hard. Finally, many foods exploited by musteloids pose less mechanical resistance: fruits and berries, fish, and small mammals are neither exceptionally hard nor tough, and thus can be exploited without significantly taxing the masticatory apparatus. Species which habitually consume tough foods (e.g., bamboo for *Ailurus fulgens*), hard foods (e.g., mollusks and sea urchins for *Enhydra lutris*), or foods that are both hard and tough (e.g., bones for *Gulo gulo*) are therefore likely to display morphological adaptations within the masticatory apparatus, which distinguish them from non-mechanically resistant feeders (Estes, 1980; Roberts and Gittleman, 1984).

Similarly, the size of exploited food and prey items (relative to the species own size) may vary drastically. Several species (mink, martens, and weasels) exploit snowshoe hares, particularly during the winter months, despite this prey often outweighing them (a typical hare may weigh 1.5 kg, a comparable mass to adult male American minks and martens). Similarly, least weasels (which weight just 100 g) regularly consume pika (which can be more than double their weight), and have even been reported to exploit animals as large as capercaillie, hazel hens, and hares (Heptner and Sludskii, 2002)—prey species that can be more than an order of magnitude larger than themselves. The exploitation of such relatively large prey might similarly impose significant demands upon the masticatory apparatus requiring exceptional gape.

Functional Myology of the Masticatory System

From an anatomical perspective, both the size and architectural configuration of the muscles of mastication are critical determinants of the functional capacity of the masticatory system. Muscle fibers are composed of functional units known as sarcomeres, which shorten to induce muscle contractions (Loeb and Ghez, 2000). As sarcomeres are serially arranged within muscle fibers, the length of its constituent fibers reflects the total excursion potential of a muscle. Within the masticatory system, this excursion potential functionally determines gape: the maximum jaw-opening potential that a species can attain. Consequently, species that exploit larger prey sizes might be expected to display an increase in fiber length (FL) (e.g., gape potential) within the masticatory musculature. Indeed, an interspecific analysis of Felidae by Hartstone-Rose et al. (2012) demonstrated that the jaw adductors of felid species, which consume relatively larger prey, possess relatively longer muscle fibers.

A second critical factor relating to masticatory performance is bite force. As sarcomeric contraction produces a muscle's intrinsic force, the total force generated during this contraction is proportional to the number of fibers arranged through the cross-sectional area of a muscle: a variable known as physiological cross-sectional area (PCSA; Close, 1972; O'Connor et al., 2005). An increase in PCSA therefore increases bite force potential; as such, species that consume mechanically challenging foods have repeatedly been shown to possess an increase in PCSA relative to taxa whose diets impose fewer mechanical challenges (Perry et al., 2011; Hartstone-Rose et al., 2012). This increase is typically facilitated by an increase in muscle volume, enhancing the number of fibers within a muscle's cross-section (Herrel et al., 2008; Taylor and Vinyard, 2009).

Masticatory Biomechanics

In addition to determining muscle architectural variables, we estimate the moment arms of each jaw adductor muscle to calculate their mechanical advantage at different bite points—a measure of the efficiency of force transfer from the muscle to a specific bite point. Mechanical advantage is measured as the ratio of a muscle's lever arm (the perpendicular distance from its line of action to the mandibular condyle; Fig. 1) and its load arm (the distance measured from the condyle to the given bite point; Fig. 2), with higher ratios reflecting a relatively elongated lever arm and describing a system in which a higher percentage of intrinsic muscle force can be transmitted to the dentition during biting (Greaves, 1980). By combining each muscle's PCSA with its mechanical advantage, we can better infer bite force and thus more closely examine the relationship between masticatory anatomy and dietary consistency.

Previous Analyses of Bite Force within the Musteloidea

Several earlier studies have sought to describe masticatory anatomy and performance within select extant (and extinct) species of Musteloid. Though much of this work has focused upon Mustelids [e.g., *Martes americana*, *Lontra canadensis*, and *Enhydra lutris* (Riley, 1985); *Enhydra lutris* (Law et al., 2016)], several other extant taxa have been analyzed from the perspective of masticatory performance, including *Procyon lotor* (Christiansen and Adolfssen, 2005; Christiansen and Wroe, 2007; Davis, 2014; Law et al., 2018), *P. cancrivorus*, *Ailurus fulgens*, *Gulo gulo*, *Taxidea taxus*, *Nasua nasua*, and others (Christiansen and Adolfssen, 2005; Christiansen and Wroe, 2007; Law et al., 2018). The feeding performance of several giant fossil mustelids (including *Megalictis*, *Eomellivora*, *Ekorus*, *Plesiogulo*, and *Enhydritherium*) has similarly been considered (Valenciano et al., 2016). However, these studies have typically relied upon combining dry-skull methods of estimating muscle volume with biomechanical proxies; consequently, data on muscle architectural variation within Musteloidea remain underreported. Moreover, while most previous studies have

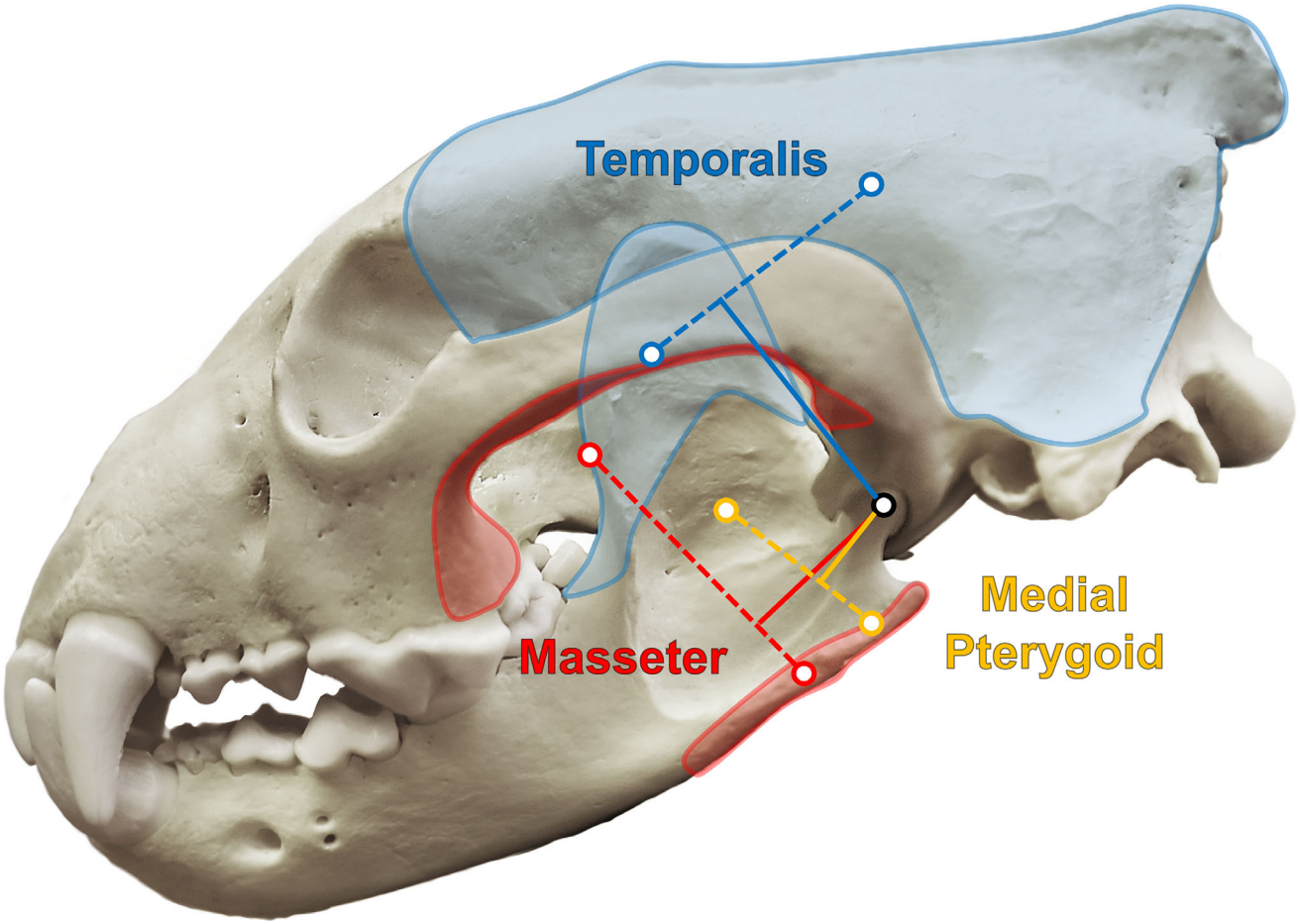

Fig. 1. Calculation of lever arm lengths within the masticatory apparatus of the wolverine (*Gulo gulo*). Shaded areas indicate muscle attachment sites (medial pterygoid attachments on deeper bony aspects not shown). Dashed colored lines indicate lines of action. Solid colored lines represent lever arm lengths for each muscle, used to calculate the mechanical advantage of each jaw adductor.

examined narrower taxonomic groups, an analysis characterizing variation in masticatory anatomy across the superfamily will allow biomechanical assessment in this carnivoran group with remarkable dietary breadth.

Aims and Predictions

This study aims to examine the masticatory apparatus of a taxonomically diverse sample of Musteloidea in relation to two dietary factors: food item size and mechanical resistance. Following previous work on the relationship between masticatory anatomy and diet in both carnivores (Hartstone-Rose et al., 2012) and other mammalian taxa (Santana et al., 2010; Perry et al., 2011; Hartstone-Rose et al., 2018), we predict that the architecture and mechanical efficiency of the jaw adductor muscles within Musteloidea will be heavily influenced by their dietary category.

Hypothesis 1: PCSA and Bite Force will scale with positive allometry relative to body size, such that larger species will be able to produce relatively larger masticatory forces. In other carnivoran lineages (Felidae and Canidae), PCSA and bite force were observed to scale with positive allometry relative to body size across a broad interspecific sample (Hartstone-Rose et al., 2012). We therefore predict that the same scaling relationship will be observed within musteloids.

Hypothesis 2: FLs will be longer in musteloids that consume relatively larger foods. Longer fibers enable greater muscle excursion and, in the jaw, increase maximum gape potential. We therefore predict that species that consume foods of a large size [relative to their own body mass (BM)] will show an increase in FL across the adductor musculature to facilitate the exploitation of relatively larger prey; a pattern previously observed within Felidae (Hartstone-Rose et al., 2012).

Hypothesis 3: PCSA and Bite Force will be higher in musteloids that eat more mechanically resistant food items. An increase in bite force capacity enables the consumption of more mechanically resistant food items (e.g., bamboo and the hard shells of mollusks). We therefore predict that species whose diets incorporate mechanically

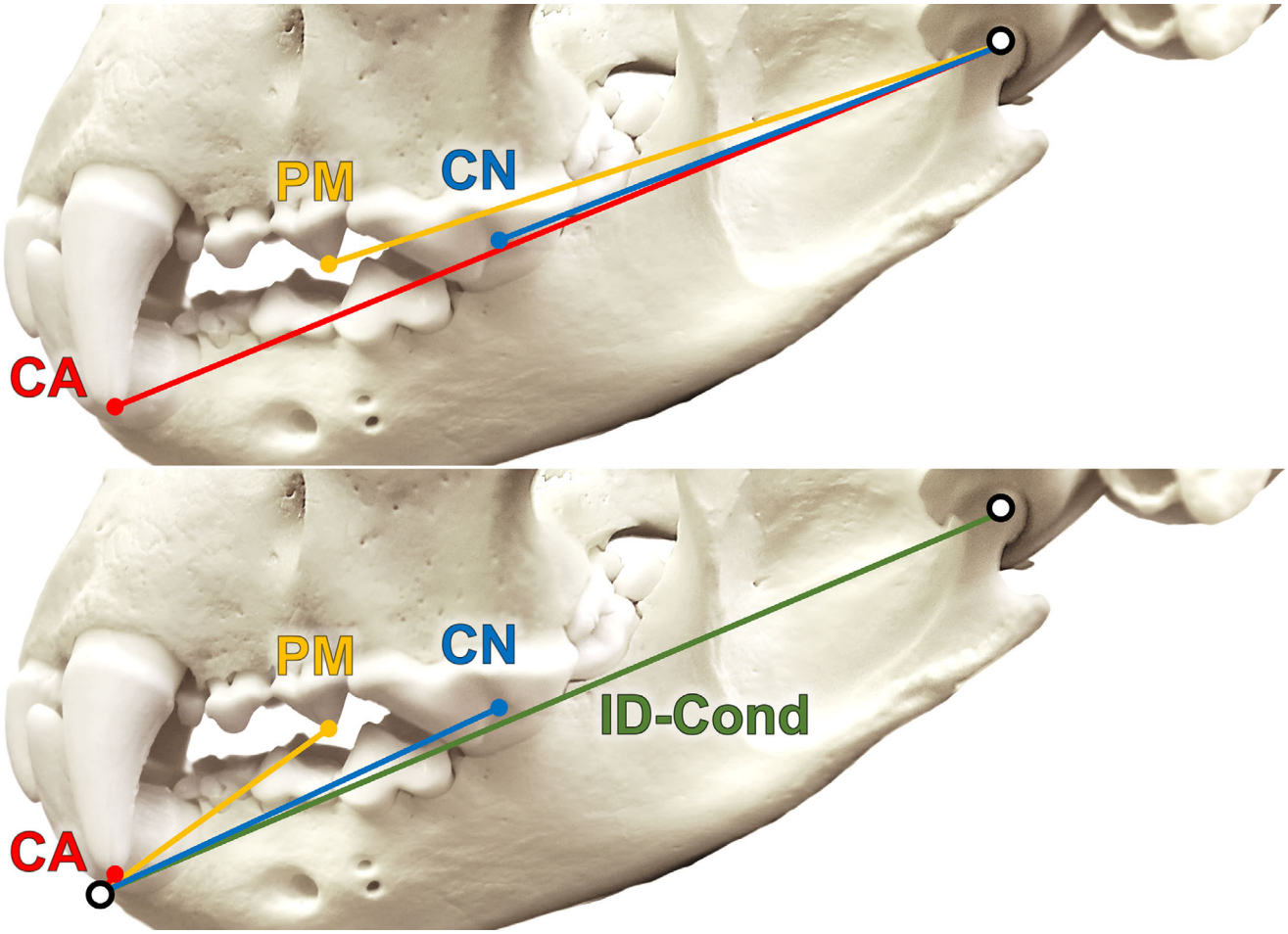

Fig. 2. Calculation of load arm lengths within the masticatory apparatus of the wolverine (*Gulo gulo*). Top image: working-side load arm lengths measured as the distance from various bite points to the fulcrum of the jaw (mandibular condyle). Bottom image: balancing-side load arm lengths measured as the distance from the mandibular condyle to the infradentale, plus the distance from the infradentale to each respective bite point.

challenging foods will display an increase in bite force potential relative to taxa whose diets consist of non-obdurate foods such as fruits and flesh.

MATERIALS AND METHODS

Sample

Our sample consisted of 17 species from the superfamily Musteloidea (Table 1). These individuals represent both wild animals (non-threatened North American species that are readily available as byproducts of the hunting/trapping/taxidermy industry) and captive specimens donated for research postmortem from various sources including the Atlanta Zoo and the Smithsonian Institution. To ensure a comprehensive sample, individuals from all four families of the superfamily Musteloidea—Ailuridae, Mephitidae, Mustelidae, and Procyonidae—were included within this study. In addition to taxonomic diversity, we similarly attempted to maximize variation in our sample across body size (including both the largest and smallest terrestrial taxa in the superfamily) and diet (with highly frugivorous, insectivorous, durophagous, and generalist taxa included for analysis).

Dietary Categorization

Species were categorized based on variation among their dietary size (DS) and their dietary mechanical properties (DMPs), using published accounts of subsistence strategies for each species (Long, 1973; Lotze and Anderson, 1979; King, 1983; Roberts and Gittleman, 1984; Clark et al., 1987; Poglayen-Neuwall and Toweill, 1988; Sheffield and King, 1994; Pasitschniak-Arts and Larivière, 1995; Smith et al., 1995; Gompper and Decker, 1998; Larivière and Walton, 1998; Kays, 1999; Larivière, 1999, 2003; Zabala and Zuberogoitia, 2003; Zhou et al., 2011; Ribas et al., 2012; Ferreira et al., 2013; Noonan et al., 2017). DS was categorized using the same method described by Hartstone-Rose et al. (2012): Species in Category 1 consume food that is mostly smaller than one order of magnitude below its own BM; species in Category 2 consume mostly food that is between one order of magnitude smaller than themselves and their own BM; species in Category 3 regularly consume prey that are larger than their own BM; and species in Category 4 derive the majority of their diet from foods that are larger than their BM (Table 1). To determine the mechanical resistance of each species' diet, each taxon was also categorized as either having a diet that is mechanically challenging/obdurate ("O") or

TABLE 1. Musteloid taxa analyzed within this study

Family	Species	Common name	Abbrev.	Sex	BM (g)	DS	DMP	Diet
Ailuridae	*Ailurus fulgens*	Red Panda	A.f.	F	4,900	1	O[b]	Herbivore
Mephitidae	*Mephitis mephitis*	Striped skunk	M.m.	U	3,075	1	S	Omnivore
Mephitidae	*Spilogale putorius*	Spotted skunk	S.p.	M	560	2	S	Omnivore
Mustelidae	*Taxidea taxus*	Badger	T.t.	U	12,020	1	S	Omnivore
Mustelidae	*Eira barbara*	Tayra	E.b.	M	4,850	2	S	Omnivore
Mustelidae	*Aonyx cinerea*	Oriental small-clawed otter	A.c.	M	3,100	2	O	Carnivore
Mustelidae	*Lontra canadensis*	River Otter	L.c.	U	9,500	2	O	Carnivore
Mustelidae	*Pteronura brasiliensis*	Giant River Otter	P.b.	U	30,000	2	O	Carnivore
Mustelidae	*Mustela erminea*	Stoat	M.e.	M	131[a]	3	S	Carnivore
Mustelidae	*Neovison vison*	Mink	N.v.	U	1,149	3	S	Carnivore
Mustelidae	*Martes americana*	Marten	M.a.	U	860	3	S	Carnivore
Mustelidae	*Mustela nivalis*	Least Weasel	M.n.	F	46	4	S	Carnivore
Mustelidae	*Gulo gulo*	Wolverine	G.g.	M	18,144[a]	4	O	Omnivore
Procyonidae	*Bassariscus astutus*	Ring Tail Cat	B.a.	M	985[a]	2	S	Carnivore
Procyonidae	*Potos flavus*	Kinkajou	P.f.	U	3,000	2	S	Omnivore
Procyonidae	*Nasua nasua*	Coati	N.n.	F	4,100	2	S	Omnivore
Procyonidae	*Procyon lotor*	Raccoon	P.l.	F	5,940	2	S	Omnivore

Abbreviations: BM, body mass; DS, dietary size; DMP, dietary mechanical properties; for sex of specimen studied, M, male; F, female; and U, unknown. Dietary size ranges from 1 to 4, with species in Category 1 consuming food that is mostly smaller than one order of magnitude below its own body mass, species in Category 2 consuming mostly food that is between one order or magnitude smaller than themselves and their own body mass, species in Category 3 regularly consuming prey that are larger than their own body mass, and species in Category 4 deriving the majority of their diet from foods that are larger than their body mass. DMP is categorized by obdurate food items (O) and soft food items (S).

[a] Indicates last living body weight used in place of literature-derived mass.

[b] Unlike the generally hard diets of the other durophages, the obdurate diet of *Ailurus fulgens*, bamboo, is fibrous and therefore tough—requiring repeated force for consumption rather than fewer high amplitude cracking forces necessitated by hard foods like shell and bone. Therefore, although they are included with other durophages in DMP (as "O"), their masticatory muscle requirements are slightly different than the other taxa in this category.

non-mechanically challenging ("S") based on published accounts of each species' diet (Table 1).

Estimation of Bite Force

For each specimen, architectural and morphometric data were collected from the jaw adductor musculature, comprising seven individual portions of three muscle groups: the superficial, deep, and zygomatic portions of the masseter and temporalis, and the medial pterygoid. In instances where high degrees of interdigitation between fibers prevented subdivision of muscle portions during excision (e.g., integration between the superficial and deep masseter), muscle groups were removed as a single block.

After removing each muscle portion (or muscle block) from its bony attachments, morphometric measurements of muscle dimensions and mass were recorded. Muscles were then subjected to a chemical digestion protocol (Herrel et al., 2008; Hartstone-Rose et al., 2012) in which each muscle was chemically digested in a 10% sulfuric acid solution at 70°C, or a 20% nitric acid solution at room temperature. As both techniques result in the same product, these techniques were used interchangeably based on chemical availability at the dissection location. Digestion times varied depending on the acid used, the amount of intrinsic connective tissue within the muscle, and the muscle's size. Once the connective tissue had been dissolved, muscle fascicles were gently separated and either measured using digital calipers or photographed alongside a scale bar and measured digitally using the software package imageJ (Version 1.51). A representative sample comprised of a minimum of 40 fibers was measured from each muscle portion. FL was used in conjunction with muscle mass (MM) to calculate the PCSA of each muscle portion using the modified formula from Schumacher (1961):

$$q = m/lp,$$

where q is PCSA (cm^2), m is MM (g), l is average FL (cm), and p is the specific density of muscle (1.0564 g/cm^3; Murphy and Beardsley, 1974). Although some colleagues "reduce" PCSA by the angles of pennation with the muscles (=RPCSA), there are several reasons that this is inadvisable in the masticatory apparatus (see Hartstone-Rose et al., 2018 for a complete discussion of masticatory PCSA vs. RPCSA). Total MM and total PCSA across the adductor complex were also calculated by summing all adductor muscle portions from each specimen. Additionally, a weighted average of FL across the adductor musculature was calculated using the formula from Hartstone-Rose et al. (2012, 2018):

$$FL_X = \frac{((FL_{MS}m_{MS}) + (FL_{TMP}m_{TMP}) + (FL_{PT}m_{PT}))}{(m_{MS} + m_{TMP} + m_{PT})}$$

where FL_X is the average FL for the jaw adductors, FL_{MS}, FL_{TMP}, and FL_{PT} are the average FLs and m_{MS}, m_{TMP}, and m_{PT} are the MMs for each respective muscle group (masseter, temporalis, and medial pterygoid respectively).

Bite force was then calculated at three different points along the tooth row: the upper canine tip, the major cusp of the third premolar, and the upper carnassial notch or its homologous equivalent in taxa that have essentially lost a true notch—the intersection of the crista of paracone and metastyle (Fig. 2). Intrinsic muscle force was calculated using each muscle's PCSA, translated into force using a previously published force constant of 25 N/cm^2 (as used in previous studies of masticatory performance, e.g., Herrel et al., 2008; Davis et al., 2010). In order to calculate leverage estimates, we took lateral photographs of

each cranium and mandible and, using ImageJ, defined the origin and insertion areas of each muscle following dissection photographs and previous descriptions of the masticatory apparatus in Carnivora (e.g., Scapino, 1968; Hartstone-Rose et al., 2012). These areas were used to calculate each muscle's lever and load arms (see Figs. 1 and 2) following Hartstone-Rose et al. (2012). Lever arms were defined as the perpendicular distance from each muscle's line of action (a vector from the centroid of its origin to the centroid of its insertion) to the fulcrum of the mandibular joint (i.e., the mandibular condyle). Load arms were defined as the distances from the condyle to each individual bite point. In order to account for both the working-side and the balancing-side of the jaw during occlusion, we assume bilateral symmetry of the specimen, such that the load arm of the balancing-side was calculated using the distance from the condyle to the infradentale, plus an additional distance from the infradentale to the balancing-side bite point (Hartstone-Rose et al., 2012).

The lever arm of each muscle (in conjunction with the load arms associated with each bite point) was used to approximate working-side bite force as follows:

$$\mathrm{WBF_{CA}} = c\left(\frac{(q_{\mathrm{MS}}L_{\mathrm{MS}}) + (q_{\mathrm{TMP}}L_{\mathrm{TMP}}) + (q_{\mathrm{PT}}L_{\mathrm{PT}})}{L_{\mathrm{CA}}}\right)$$
$$\mathrm{WBF_{PM}} = c\left(\frac{(q_{\mathrm{MS}}L_{\mathrm{MS}}) + (q_{\mathrm{TMP}}L_{\mathrm{TMP}}) + (q_{\mathrm{PT}}L_{\mathrm{PT}})}{L_{\mathrm{PM}}}\right)$$
$$\mathrm{WBF_{CN}} = c\left(\frac{(q_{\mathrm{MS}}L_{\mathrm{MS}}) + (q_{\mathrm{TMP}}L_{\mathrm{TMP}}) + (q_{\mathrm{PT}}L_{\mathrm{PT}})}{L_{\mathrm{CN}}}\right),$$

where $\mathrm{WBF_{CA}}$, $\mathrm{WBF_{PM}}$, and $\mathrm{WBF_{CM}}$ represent working-side bite force at the canine, premolar, and carnassial, respectively; c represents the force constant of 25 N/cm^2 (as above); q_{MS}, q_{TMP}, and q_{PT} represent the PCSA values of the masseter, medial pterygoid, and temporalis; L_{MS}, L_{TMP}, and L_{PT} represent lever arm lengths of the masseter, temporalis, and medial pterygoid, respectively; and L_{CA}, L_{PM}, and L_{CN} represent the load arm lengths of the moment arms from each bite point.

A similar approach was applied to calculate balancing-side bite force, in which the lever arms of each muscle were combined with balancing-side load arms (Fig. 2) using the following formula:

$$\mathrm{BBF_{CA}} = c\left(\frac{(q_{\mathrm{MS}}L_{\mathrm{MS}}) + (q_{\mathrm{TMP}}L_{\mathrm{TMP}}) + (q_{\mathrm{PT}}L_{\mathrm{PT}})}{L'_{\mathrm{CA}}}\right)$$
$$\mathrm{BBF_{PM}} = c\left(\frac{(q_{\mathrm{MS}}L_{\mathrm{MS}}) + (q_{\mathrm{TMP}}L_{\mathrm{TMP}}) + (q_{\mathrm{PT}}L_{\mathrm{PT}})}{L'_{\mathrm{PM}}}\right)$$
$$\mathrm{BBF_{CN}} = c\left(\frac{(q_{\mathrm{MS}}L_{\mathrm{MS}}) + (q_{\mathrm{TMP}}L_{\mathrm{TMP}}) + (q_{\mathrm{PT}}L_{\mathrm{PT}})}{L'_{\mathrm{CN}}}\right),$$

where $\mathrm{BBF_{CA}}$, $\mathrm{BBF_{PM}}$, and $\mathrm{BBF_{CN}}$ represent working-side bite force at the canine, premolar, and carnassial, respectively; c represents the force constant of 25 N/cm^2 (as above); q_{MS}, q_{TMP}, and q_{PT} represent the PCSA values of the masseter, medial pterygoid, and temporalis; L_{MS}, L_{TMP}, and L_{PT} represent lever arm lengths of the masseter, temporalis, and medial pterygoid, respectively; and L'_{CA}, L'_{PM}, and L'_{CN} represent the balancing-side load arm lengths for each bite point (Fig. 2). Total BF is subsequently calculated by the sum of forces produced by the balancing and working side.

To analyze relative bite force across our sample, two different proxies were used to estimate body size: BM and geometric mean (GM). The BM for each individual measured as the last living weight of the specimen (or sex-specific adult masses described in the literature when the individual's last living BM was not known), while GM was established through craniometric measurements of the specimens' skulls following Hartstone-Rose et al. (2012). The following craniometrics measurements were used to calculate GM: cranial length (measured in the midsagittal plane from the inion to interdentale), cranial height (measured as the highest point on the frontal bone to the posterior edge of the palate), jaw length (measured from the posterior edge of the condyle to the infradentale), jaw height (measured in the coronal plane from the lower carnassial notch [or homologous point] to the inferior border of the mandible), jaw width (measured at a point directly inferior to the carnassial), bizygomatic

TABLE 2. Masticatory muscle masses (g), fiber lengths (mm), and PCSA values (cm^2) for each species within this study

Species name	Temporalis mass (g)	Temporalis FL (mm)	Temporalis PCSA (cm^2)	Masseter mass (g)	Masseter FL (mm)	Masseter PCSA (cm^2)	Medial pterygoid mass (g)	Medial pterygoid FL (mm)	Medial pterygoid PCSA (cm^2)
Ailurus fulgens	36.34	19.58	17.57	10.42	15.47	6.38	4.51	13.62	3.13
Mephitis mephitis	9.70	9.53	9.64	2.40	5.83	3.90	0.70	4.86	1.36
Spilogale putorius	3.91	10.41	3.55	0.98	3.83	2.41	0.34	3.055	1.06
Taxidea taxus	27.1	10.4	24.67	7.6	10.09	7.13	1.80	6.43	2.65
Eira barbara	10.42	12.2	8.08	3.65	8.67	3.99	1.65	6.9	2.26
Aonyx cinerea	12.54	12.72	9.33	3.15	12.4	2.40	0.49	6.23	0.74
Lontra canadensis	24.32	18.74	12.28	6.95	11.66	5.64	0.89	8.2	1.03
Pteronura brasiliensis	161.53	25.62	59.69	22.6	14.19	15.08	4.5	8.93	4.77
Mustela erminea	0.58	7.74	0.71	0.09	1.54	0.55	0.08	3.52	0.22
Neovison vison	3.15	12.38	2.41	0.69	5.89	1.11	0.12	4.84	0.23
Martes americana	4.78	10.7	4.23	1.52	8.09	1.78	0.3	5.27	0.54
Mustela nivalis	0.27	7.6	0.34	0.05	3.3	0.14	0.07	4.1	0.16
Gulo gulo	128.13	20.12	60.28	30.09	14.25	19.99	5.29	11.42	4.38
Bassariscus astutus	6.49	9.67	6.35	2.12	8.41	2.39	0.52	4.6	1.07
Potos flavus	8.55	11.47	7.06	3.10	8.2	3.58	0.46	4.219	1.03
Nasua nasua	12.398	10.49	11.18	5.82	9.2	5.99	1.26	5.62	2.12
Procyon lotor	19.89	15.67	12.02	8.4	10.1	7.87	1.2	7.71	1.47

breadth (measured between the lateral surfaces of the zygomatic arches at their widest points), orbital height (measured from the most inferior to most superior point of the orbital socket), and orbital width (measured from the most lateral to most medial point of the orbital socket, directly perpendicular to orbital height). The product of these values was taken to the eighth root to calculate GM.

Prior to analysis, all data were linearized (i.e., cubic and square roots were taken of the volumetric and area variables, respectively) and log-transformed, such that isometric slopes were transformed to 1 for all variables. The BF at each bite point was analyzed using reduced major axis (RMA) regressions against both BM and GM, and residuals were analyzed using *t*-tests to determine statistical significance between functional groups.

RESULTS

Scaling of Adductor Properties

Full architectural data for each specimen are presented in Table 2. RMA regressions of total adductor MM against BM (Fig. 3) resulted in an isometric slope of 0.954 (95% CI = 0.829–1.10). Total PCSA scaled with positive allometry against BM (slope of 1.16, 95% CI = 1.00–1.34), as did bite force at all three measured bite points (Table 3), supporting Hypothesis 1. Finally, weighted FLs scaled with negative allometry relative to BM across our entire sample (slope of 0.64, 95% CI = 0.43–0.95).

The same masticatory variables scaled relative to cranial GM (Fig. 4) resulted in positive allometry for total adductor MM (slope of 1.22, 95% CI = 1.06–1.40) and PCSA (slope of 1.48, 95% CI = 1.31–1.67). Lastly, the weighted FLs scaled with isometry against GM, albeit with wide confidence intervals (slope of 0.82, 95% CI = 0.53–1.28).

Dietary Size

Regression of FL residuals from RMA regression against BM against dietary category revealed a correlation between DS and adductor FLs. While sample sizes were sufficiently small as to preclude robust statistical comparison, a fit of ordinary least squares regression line for the entire sample yielded an r^2 value of 0.25 (Fig. 5). Exclusion of the anomalous red panda increased this correlation to 0.56 (Fig. 5). When scaled against the residuals of FL against cranial GM, this regression yields r^2 values of 0.25 and 0.39 (with the inclusion and exclusion of the red panda, respectively). Furthermore, a two-tailed *t*-test between grouped categories of small (DS = 1 and 2) and large (DS = 3 and 4) food consumers demonstrated that species consuming relatively small foods had shorter FLs than species consuming relatively large foods ($P = 0.0154$). Collectively, these analyses support our initial prediction that musteloids that consume larger foods will demonstrate increased FLs (Hypothesis 2).

Dietary Mechanical Properties

Bite force data for each taxon at bite points along the dental row are presented in Table 4 and Figures 6 and 7. Relative to BM, neither bite force (at any bite point) nor PCSA differed significantly between musteloids that consume "soft" and "obdurate" diets (Table 5; $P = 0.54$–0.88), contrary to the prediction of Hypothesis 3. When comparing PCSA and bite force against GM, the same nonsignificant trend was observed (Table 5; $P = 0.24$–0.31).

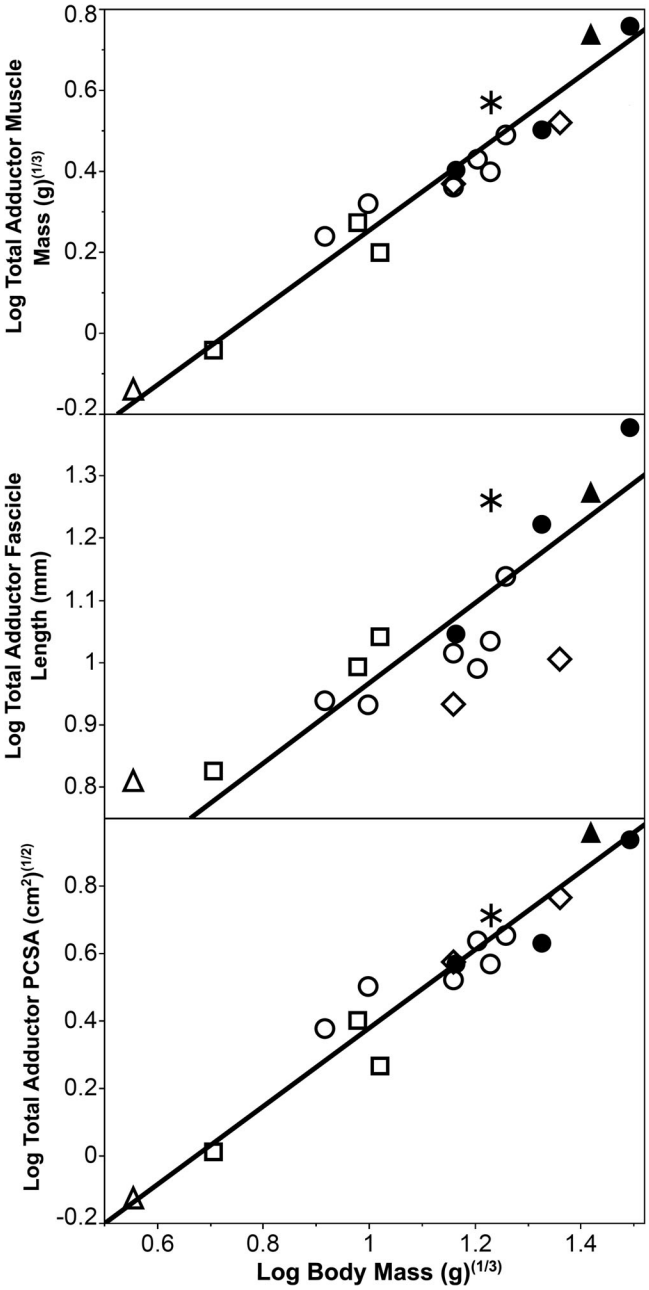

Fig. 3. Reduced major axis regression of myological variables (muscle mass, fiber length, and PCSA) against body mass. Both variables are log-transformed. Dietary sizes represented by symbols: diamonds = size 1, circles = size 2, squares = size 3, triangles = size 4, asterisk = red panda. Filled symbols indicate obdurate diet and unfilled symbols indicate non-obdurate diet.

DISCUSSION

Comparisons to Previous Estimations of Bite Force within the Musteloidea

As noted above, previous work has attempted to estimate bite force potential within several Musteloid taxa through the use of dry-skull correlates. Such data are reported for three Mustelid taxa (*Meles meles*, *Taxidea*

taxus, and *Gulo gulo*), three Procyonid taxa (*Nasua nasua*, *Procyon lotor*, *and Procyon cancrivorus*), and the sole species of Ailurid (*Ailurus fulgens*) by Christiansen and Adolfssen (2005). Of these seven species, five taxa overlap with our own data set. Overall, our dissection-derived estimates of bite force potential closely correspond to dry-skull estimates: for example, in *Taxidea taxus*, at the carnassial and canine tooth, respectively, we calculated potential bite forces of 354.45 N and 236.3 N, data that closely matched predictions of 322.9 N at 217.9 N by Christiansen and Adolfssen (2005). Similarly, good correspondence exists for *Ailurus fulgens* and *Procyon lotor*. However, both *Nasua nasua* and *Gulo gulo* display significantly greater estimates of bite force within our own study at both the carnassial and canine (134.59 N and 88.11 N vs. 87.1 N and 53.2 N for *Nasua nasua*, and 1,091.37 N and 640.16 N vs. 408.3 N and 254.3 N for *Gulo gulo*). It is expected that a major contributor toward these differences would be the starkly different methodologies employed by these studies; however, in the case of *Gulo gulo*, it should also be noted that our specimen appeared toward the larger end for the species (last living body weight of 18.1 kg), which may partially contribute to our greater estimates of bite force. Furthermore, an earlier report of dry-skull estimated bite force in the wolverine by Wiersma (2001) estimates a maximum bite force of 844.88 N at the anterior dentition, a magnitude much more closely aligned to our own estimate.

Finally, the most comprehensive comparative data set for bite force within Musteloidea is reported by Christiansen and Wroe (2007). Again using dry-skull methods, they report estimated bite forces at both the canine and carnassial tooth for 13 of the 17 taxa analyzed within this study. These data generally show good agreement with our own: for example, bite forces of 71.94 N and 109.53 N versus 73.3 N and 99.9 N at the canine and carnassial teeth, respectively, of *Mephitis mephitis*; however, four taxa (*Eira barbara*, *Gulo gulo*, *Mustela erminea*, and *Mustela nivalis*) show relatively large divergences, which may again be attributed to methodological differences and variation in specimen size and/or sex. Nonetheless, the generally strong agreement that exists between these three previous studies and our own suggests that dry-skull and dissection-derived methods for estimating bite forces within musteloids appear comparable, though not directly interchangeable. Given that the fascicular approach to bite force estimation incorporates substantially more functional variables (including both the motor and leverage components of the system), we think that these estimates are closer to the behavioral reality though they clearly take a more intensive, time-consuming, and destructive approach to their calculation.

Scaling of Architectural Properties within the Musteloidea

Jaw adductor MM scaled isometrically against BM and with slight positive allometry against GM. These results mirror trends seen in the jaw adductors of Felids (Hartstone-Rose et al., 2012) and within Canids (Penrose et al., 2016). Weighted FLs scaled with negative allometry against both size variables, which is also consistent with the results of felid jaw adductor FL. Finally, PCSA scaled

TABLE 3. Reduced-major axis (RMA) regression statistics of masticatory variables and bite force potential against body mass

	Against body mass			Against cranial geometric mean			
y-variable	Slope	*y*-intercept	r	95% CI	Slope	*y*-intercept	r	95% CI
Log masseter mass (g) 1/3	1.01	−1	0.9668	0.87–1.17	1.30	−1.66	0.98	1.18–1.43
Log temp mass (g) 1/3	0.96	−0.75	0.967	0.83–1.11	1.23	−1.38	0.96	1.06–1.43
Log MP mass (g) 1/3	0.78	−0.93	0.894	0.59–1.04	1.00	−1.45	0.92	0.79–1.27
Log total adductor mass 1/3	0.95	−0.7	0.969	0.83–1.10	1.22	−1.32	0.97	1.06–1.40
Log average FL	0.64	0.32	0.828	0.43–0.95	0.82	−0.1	0.80	0.53–1.28
Log total PCSA 1/2	1.16	−0.78	0.967	1–1.34	1.48	−1.54	0.98	1.31–1.67
Log BF Ca 1/2	1.19	−0.76	0.962	1.02–1.40	1.53	−1.54	0.96	1.28–1.81
Log BF P3 1/2	1.18	−0.72	0.961	1–1.38	1.50	−1.49	0.95	1.27–1.79
Log BF Carn 1/2	1.16	−0.67	0.959	0.98–1.37	1.48	−1.43	0.95	1.24–1.77

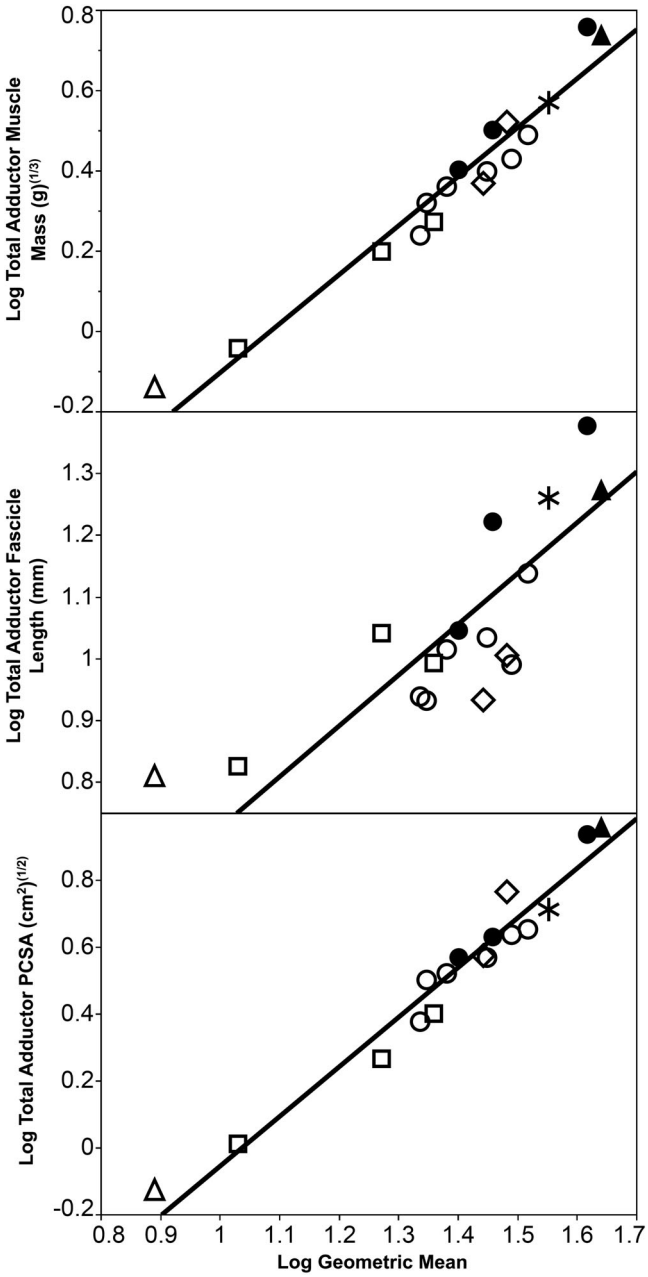

Fig. 4. Reduced major axis regression of myological variables (muscle mass, fiber length, and PCSA) against cranial geometric mean. Both variables are log-transformed. Dietary sizes represented by symbols: diamonds = size 1, circles = size 2, squares = size 3, triangles = size 4, asterisk = red panda. Filled symbols indicate obdurate diet and unfilled symbols indicate non-obdurate diet.

with significant positive allometry against both BM and GM, with strongly comparable slopes to those reported within Felidae (Hartstone-Rose et al., 2012). However, this slope differs to previous reports of scaling across a more taxonomically diverse Carnivoran sample (which included canids, felids, herpestids, ursids, viverids, and musteloids). Across this wider range, smaller species were reported to possess relatively elevated bite forces, such that PCSA

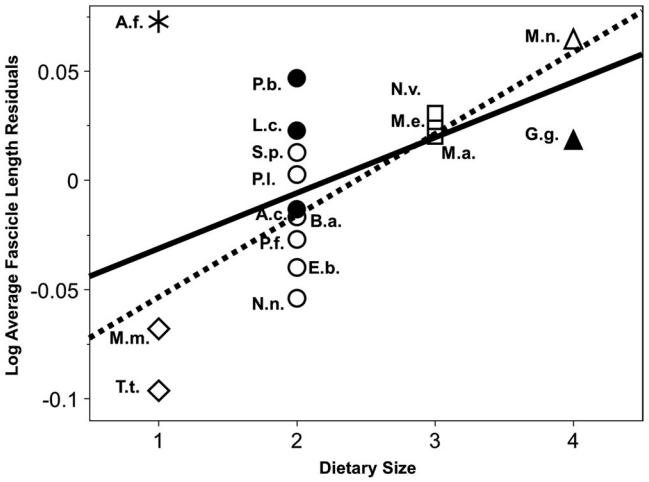

Fig. 5. Residuals of RMA regression of fiber length against body mass, organized by dietary size. Filled symbols indicate obdurate diet and unfilled symbols indicate non-obdurate diet. See Table 1 for abbreviations.

scaled with negative allometry relative to body size (Christiansen and Wroe, 2007).

Food Item Size and Masticatory Anatomy within the Musteloidea

The dietary range of Musteloidea is notably diverse, spanning dedicated frugivory, folivory, insectivory, and durophagy. Despite this diversity, a clear trend between food item size and FLs (a key architectural determinant of gape potential) is apparent, supporting Hypothesis 2. Species which consume relatively larger foods (e.g., DS Categories 3 and 4) demonstrate significantly longer muscle fiber ($P = 0.0154$) across the masticatory musculature than those consuming smaller food items. These data suggest that increased FLs across the adductor musculature may be a key adaptation toward permitting the exploitation of larger prey. Previous research has also demonstrated this same trend within Felids (Hartstone-Rose et al., 2012); the observation of this same trend within the Musteloidea therefore suggests that the functional relationship between FLs and prey size may be more universal than previously recognized. Further, as similar trends are also known within non-carnivorous taxa (e.g., Callitrichid primates, wherein gouging gummivorous species who frequently utilize wide gapes demonstrate longer fiber than non-gouging taxa; Taylor et al. (2009)), the link between FLs and gape requirements appears to be consistently strong across the mammalian adductor musculature. This trend is best exemplified in the least weasel (*Mustela nivalis*), the world's smallest carnivore, which often consumes prey more than one order of magnitude greater in BM than itself (Sheffield and King, 1994; Heptner and Sludskii, 2002). As a result, the least weasel displayed the second strongest positive residuals for FL when scaled against BM data (second only to the formidably wolverine), demonstrating the anatomical adaptations which facilitate the least weasels' impressive capacity to exploit prey much larger than itself.

TABLE 4. Combined biomechanical and myological estimates of total bite force (Newton) across Musteloidea, measured at three bite points along the dental row

Family	Species name	Bite force at carnassial notch (N)	Bite force at P3 (N)	Bite force at canine (N)
Ailuridae	*Ailurus fulgens*	274.02	228.75	182.81
Mephitidae	*Mephitis mephitis*	109.53	84.75	71.94
Mephitidae	*Spilogale putorius*	50.75	35.16	28.76
Mustelidae	*Taxidea taxus*	354.45	294.41	236.30
Mustelidae	*Eira barbara*	132.70	106.33	83.45
Mustelidae	*Aonyx cinerea*	103.83	93.17	84.00
Mustelidae	*Lontra canadensis*	153.14	117.66	90.31
Mustelidae	*Pteronura brasiliensis*	852.68	672.20	532.12
Mustelidae	*Mustela erminea*	13.83	10.28	7.96
Mustelidae	*Neovison vison*	35.16	25.88	19.94
Mustelidae	*Martes americana*	63.38	49.01	34.88
Mustelidae	*Mustela nivalis*	6.49	5.05	3.71
Mustelidae	*Gulo gulo*	1,091.37	851.13	640.16
Procyonidae	*Bassariscus astutus*	77.09	65.21	46.67
Procyonidae	*Potos flavus*	120.41	103.98	82.31
Procyonidae	*Nasua nasua*	134.59	122.83	88.11
Procyonidae	*Procyon lotor*	149.23	135.64	102.98

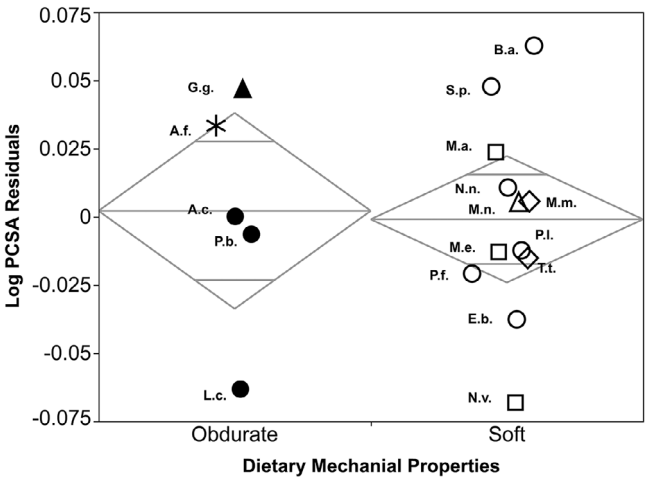

Fig. 6. Residuals of RMA regression of adductor PCSA against body mass, organized by dietary mechanical resistance. Dietary sizes represented by symbols: diamonds = size 1, circles = size 2, squares = size 3, triangles = size 4, asterisk = red panda. See Table 1 for abbreviations.

Despite this seemingly robust relationship between food item size and FL, the longest adductor fibers (relative to BM) within our masticatory sample were observed within the red panda *(Ailurus fulgens)*—a bamboo specialist consuming among the smallest foods (DS Category 1) within our sample. While the functional justification for the anomalous nature of FLs within this taxon is unclear, one possible explanation for this oddity may be the red panda is overbuilt within the craniofacial region relative to other Musteloidea, such that all masticatory variables appear large relative to BM. This is supported both by the similarly positive scaling of MM and PCSA within this taxon relative to BM (Fig. 3), and the observation that, when variables are regressed against cranial GM as opposed to BM, the red panda aligns more closely to our whole-sample regression lines (Fig. 4).

Bite Force and Diet within the Musteloidea

By contrast, the relationship between bite force and diet across the Musteloidea appears less well established. As might be expected, our tough food specialist (the red panda) displayed significant positive residuals in terms of PCSA, implying a relatively high bite force for its BM (Fig. 6). This observation supports the earlier findings of Christiansen and Wroe (2007), who note that both the red panda and the giant panda (*Ailuropoda melanoleuca*) display significantly elevated bite forces relative to their body size. This trend is interpreted to reflect a specialization among dedicated herbivorous carnivorans toward the tough nature of their diet. However, across our entire sample (both when adjusted for BM or cranial GM), total adductor PCSA was not significantly greater within taxa, which consume mechanically challenging foods than those with non-obdurate diets, contrary to Hypothesis 3. Indeed, while the two most strongly durophagous taxa (the wolverine and giant river otter) displayed the greatest absolute PCSA values, both plot on or near the whole-sample regression line when adjusted for body and/or cranial size.

It is possible that, unlike FL (which appears to closely track food item size), the bite force of a species may be subject to more diverse ecological pressures than food item toughness/hardness alone. While many Musteloid taxa are carnivorous, few are apex predators. Many mustelids, in particular, are preyed upon by both terrestrial (e.g., foxes) and aerial (e.g., raptors) predators (Long, 1973; Lotze and Anderson, 1979; King, 1983). Consequently, the ability to generate high bite forces might be frequently necessitated during predation defense. This requirement for high bite force might additionally explain previous interpretations of the masticatory apparatus of musteloids by Law et al. (2018), who note that musteloids exhibit evolutionary shifts toward a larger head size, an important adaptation toward accommodating larger and more powerful masticatory musculature.

Finally, while no statistically significant differences in overall mechanical advantage were observed between Musteloid taxa consuming soft and hard/tough diets of Musteloidea, it is also interesting to note that mechanical advantage for the temporalis and masseter was consistently greater in the Musteloids within the obdurate food items category, while the mechanical advantage of medial pterygoid was higher in the

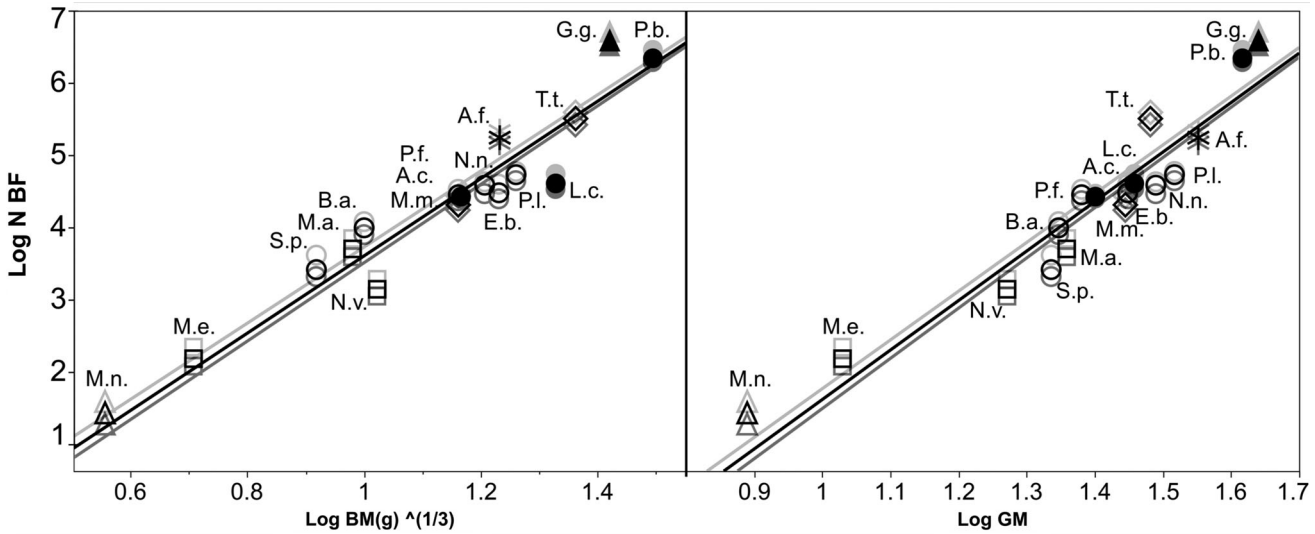

Fig. 7. Reduced major axis regressions of bite force (BF) at three bite points (canine, P3, and carnassial) against body mass and geometric mean within Musteloidea. All variables are log-transformed. Light gray = BF at the carnassial; Black = BF at the P3; Dark gray = BF at the canine.

TABLE 5. T-test significance values resulting from regressions of PCSA and bite force residuals at each of three bite points (canine, P3, and carnassial) against body mass and cranial geometric mean between musteloids with soft and obdurate diets

Size proxy	Masticatory Force Variable	*P*-values
Body mass	PCSA	0.88
	BF at canine	0.54
	BF at P3	0.59
	BF at carnassial	0.57
Cranial geometric mean	PCSA	0.31
	BF at canine	0.24
	BF at P3	0.27
	BF at carnassial	0.26

All variables were log-transformed prior to regression.

Musteloids within the soft food items category. These data may suggest distinct functional roles within the adductor complex of Musteloids during the processing of different food items, an observation which future studies may wish to explore through the use of electromyography (as explored in primates; e.g., Hylander et al., 2005; Wall et al., 2006).

Phylogenetic Variation in Bite Force within Musteloidea

In the family Ailuridae, the extant red panda, as expected, demonstrated positive residuals for bite force at all bite points. As discussed above, the high bite force capabilities of the red panda likely represent a necessary adaptation for shearing its tough, bamboo-dominated diet (Christiansen and Wroe, 2007). The family Mephitidae closely followed our whole-group regression line, with the spotted skunk showing slight positive residuals for bite force and the striped skunk slight negative residuals. Within the Procyonidae, all taxa displayed negative residuals with the exception of the ringtail (*Bassariscus astutus*), which fell slightly above our regression line. Finally, the Mustelidae, the most taxonomically diverse family within the group, showed extreme variability, including the taxon with the strongest positive residuals (the wolverine, *Gulo gulo*) and the two taxa with the strongest negative residuals (the marten, *Neovison vison* and the river otter, *Lontra canadensis*). While two of these taxa follow predictable dietary trends (the wolverine possesses a mechanically challenging diet, while the marten exploits predominantly non-challenging foods), the combination of low relative bite force and obdurate DMPs in the river otter defied our expectations. Moreover, the other two otters analyzed within this study (the giant river otter and Asian small-clawed otter) plot only slightly above and slightly below our whole-sample regression line. It would therefore appear that, across the otters analyzed within our sample, there is no strong signal for high relative bite force, such that the masticatory apparatus of these taxa might more closely reflect the major component of piscivory within their diet than the minor component of obdurate mollusk and crustacean exploitation. This finding supports an earlier hypothesis proposed by Christiansen and Wroe (2007), who observed that, among mustelids, piscivorous taxa had relatively decreased bite forces than terrestrial carnivores; a finding which they interpreted to reflect the increased mechanical resistance of mammalian and reptilian prey relative to fish.

Summary/Conclusions

The superfamily Musteloidea encompasses a broad spectrum of dietary niches, and exhibits significant variation in both BM and cranial size. However, the relationship between masticatory anatomy and dietary category appears to vary considerably. While FLs appear to strongly reflect food item size (a trend previously observed within Felids), no directional relationship can be observed between bite force potential and food mechanical resistance. This may reflect the fact that the retention of a high bite force capacity may serve other ecological functions, such as predation defense.

Collectively, the strong similarity between these data and findings previously reported within the Felidae suggest that the mechanisms by which masticatory anatomy can be seen to reflect dietary ecology may be more universally consistent across carnivores than previously recognized.

ACKNOWLEDGEMENTS

We would like to thank our editor Tim Smith and our reviewers for their valuable comments and assistance during the preparation of this manuscript. In particular, Alberto Valenciano provided extremely detailed and constructive feedback on this manuscript that greatly improved its final state. Additionally, we are grateful to Jillian Davis, the North Carolina Museum of Natural Sciences, the Philadelphia Zoo, the Smithsonian, and Zoo Atlanta for providing some of the rarer specimens in our sample. This work was funded, in part, by the National Science Foundation (IOS-15-57125).

LITERATURE CITED

Alves-Costa CP, Da Fonseca GA, Christófaro C. 2004. Variation in the diet of the brown-nosed coati (*Nasua nasua*) in southeastern Brazil. J Mammal 85:478–482.

Berthaume MA. 2016. Food mechanical properties and dietary ecology. Am J Phys Anthropol 159:79–104.

Christiansen P, Adolfssen JS. 2005. Bite forces, canine strength and skull allometry in carnivores (Mammalia, Carnivora). J Zool 266: 133–151.

Christiansen P, Wroe S. 2007. Bite forces and evolutionary adaptations to feeding ecology in carnivores. Ecol Lett 88:347–358.

Clark TW, Anderson E, Douglas C, Strickland M. 1987. Martes americana. Mamm Species 289:1–8.

Close R. 1972. Dynamic properties of mammalian skeletal muscles. Physiol Rev 52:129–197.

Constantino PJ, Lee JJ-W, Morris D, Lucas PW, Hartstone-Rose A, Lee W-K, Dominy NJ, Cunningham A, Wagner M, Lawn BR. 2011. Adaptation to hard-object feeding in sea otters and hominins. J Hum Evol 61:89–96.

Dalerum F, Kunkel K, Angerbjörn A, Shults BS. 2009. Diet of wolverines (*Gulo gulo*) in the western Brooks Range, Alaska. Polar Res 28:246–253.

Davis JS. 2014. Functional morphology of mastication in musteloid carnivorans. PhD Dissertation, Ohio University.

Davis JL, Santana SE, Dumont ER, Grosse IR. 2010. Predicting bite force in mammals: two-dimensional versus three-dimensional lever models. J Exp Biol 213:1844–1851.

Donadio E, Di Martino S, Aubone M, Novaro AJ. 2004. Feeding ecology of the Andean hog-nosed skunk (*Conepatus chinga*) in areas under different land use in north-western Patagonia. J Arid Environ 56:709–718.

Dragoo JW, Sheffield SR. 2009. *Conepatus leuconotus* (Carnivora: Mephitidae). Mamm Species 827:1–8.

Estes J. 1980. *Enhydra lutris*. Mamm Species 133:1–8.

Ferreira GA, Nakano-Oliveira E, Genaro G, Lacerda-Chaves AK. 2013. Diet of the coati *Nasua nasua* (Carnivora: Procyonidae) in an area of woodland inserted in an urban environment in Brazil. Rev Chil Hist Nat 86:95–102.

Gatti A, Bianchi R, Rosa CRX, Mendes SL. 2006. Diet of two sympatric carnivores, *Cerdocyon thous* and *Procyon cancrivorus*, in a restinga area of Espirito Santo State, Brazil. J Trop Ecol 22:227–230.

Gompper ME, Decker DM. 1998. *Nasua nasua*. Mamm Species 580:1–9.

Goswami A. 2006. Morphological integration in the Carnivoran skull. Evolution 60:169–183.

Greaves WS. 1980. The mammalian jaw mechanism–the high glenoid cavity. Am Nat 116:432–440.

Hartstone-Rose A, Perry JM, Morrow CJ. 2012. Bite force estimation and the fiber architecture of felid masticatory muscles. Anat Rec 295:1336–1351.

Hartstone-Rose A, Deutsch AR, Leischner CL, Pastor F. 2018. Dietary correlates of masticatory muscle fiber architecture in primates. Anat Rec 301:311–324.

Heptner V, Sludskii A. 2002. *Mammals of the Soviet Union. Vol. II, part 1b, Carnivores (Mustelidae and Procyonidae)*. Washington, DC: Smithsonian Institution Libraries and National Science.

Herrel A, De Smet A, Aguirre LF, Aerts P. 2008. Morphological and mechanical determinants of bite force in bats: do muscles matter? J Exp Biol 211:86–91.

Hill DA, Lucas PW. 1996. Toughness and fiber content of major leaf foods of Japanese macaques (*Macaca fuscata* yakui) in Yakushima. Am J Primatol 38:221–231.

Hylander WL, Wall CE, Vinyard CJ, Ross CF, Ravosa MJ, Williams SH, Johnson KR. 2005. Temporalis function in anthropoids and strepsirrhines: an EMG study. Am J Phys Anthropol 128:35–56.

Kays RW. 1999. Food preferences of Kinkajous (*Potos flaws*): A frugivorous carnivore. J Mammal 80:589–599.

King CM. 1983. *Mustela erminea*. Mamm Species 195:1–8.

Larivière S. 1999. *Mustela vison*. Mamm Species 608:1–9.

Larivière S. 2003. *Amblonyx cinereus*. Mamm Species 720:1–5.

Larivière S, Walton LR. 1998. *Lontra canadensis*. Mamm Species 587:1–8.

Law CJ, Young C, Mehta RS. 2016. Ontogenetic scaling of theoretical bite force in southern sea otters (*Enhydra lutris nereis*). Physiol Biochem Zool 89:347–363.

Law CJ, Duran E, Hung N, Richards E, Santillan I, Mehta RS. 2018. Effects of diet on cranial morphology and biting ability in musteloid mammals. J Evol Biol 31:1918–1931.

Loeb GE, Ghez C. 2000. The motor unit and muscle action. *Principles of neural science*, Vol. 380. New York: McGraw-Hill. p 674–694.

Long CA. 1973. *Taxidea taxus*. Mamm Species 26:1–4.

Lotze J-H, Anderson S. 1979. *Procyon lotor*. Mamm Species 119:1–8.

Montalvo CI, Pessino ME, Bagatto FC. 2008. Taphonomy of the bones of rodents consumed by Andean hog-nosed skunks (*Conepatus chinga*, Carnivora, Mephitidae) in central Argentina. J Archaeol Sci 35:1481–1488.

Murphy R, Beardsley AC. 1974. Mechanical properties of the cat soleus muscle in situ. Am J Physiol 227:1008–1013.

Noonan P, Prout S, Hayssen V. 2017. *Pteronura brasiliensis* (Carnivora: Mustelidae). Mamm Species 953:97–108.

O'Connor CF, Franciscus RG, Holton NE. 2005. Bite force production capability and efficiency in Neandertals and modern humans. Am J Phys Anthropol 127:129–151.

Pasitschniak-Arts M, Larivière S. 1995. *Gulo gulo*. Mamm Species 499:1–10.

Penrose F, Kemp GJ, Jeffery N. 2016. Scaling and accommodation of jaw adductor muscles in Canidae. Anat Rec 299:951–966.

Perry JM, Hartstone-Rose A, Wall CE. 2011. The jaw adductors of strepsirrhines in relation to body size, diet, and ingested food size. Anat Rec 294:712–728.

Poglayen-Neuwall I, Toweill DE. 1988. *Bassariscus astutus*. Mamm Species 327:1–8.

Ribas C, Damasceno G, Magnusson W, Leuchtenberger C, Mourão G. 2012. Giant otters feeding on caiman: evidence for an expanded trophic niche of recovering populations. Stud Neotrop Fauna Environ 47:19–23.

Riley MA. 1985. An analysis of masticatory form and function in three mustelids *(Martes americana*, *Lutra canadensis*, *Enhydra lutris*). J Mammal 66:519–528.

Roberts MS, Gittleman JL. 1984. *Ailurus fulgens*. Mamm Species 222:1–8.

Santana SE, Dumont ER, Davis JL. 2010. Mechanics of bite force production and its relationship to diet in bats. Funct Ecol 24: 776–784.

Scapino RP. 1968. Biomechanics of feeding in Carnivora. PhD Dissertation, University of Illinois.

Schumacher GH. 1961. *FunktionelleMorphologie der Kaumuskulatur*. Jena: Fisher.

Sheffield SR, King CM. 1994. *Mustela nivalis*. Mamm Species 454:1–10.

Smith G, Ragg J, Moller H, Waldrup K. 1995. Diet of feral ferrets (*Mustela furo*) from pastoral habitats in Otago and Southland, New Zealand. N Z J Zool 22:363–369.

Taylor AB, Vinyard CJ. 2009. Jaw-muscle fiber architecture in tufted capuchins favors generating relatively large muscle forces without compromising jaw gape. J Hum Evol 57: 710–720.

Taylor AB, Eng CM, Anapol FC, Vinyard CJ. 2009. The functional correlates of jaw-muscle fiber architecture in tree-gouging and nongouging callitrichid monkeys. Am J Phys Anthropol 139: 353–367.

Valenciano A, Leischner CL, Grant A, Abella J, Hartstone-Rose A. 2016. Preliminary bite force estimations of Miocene giant mustelids (Carnivora, Mustelidae). In: 11th International Congress of Vertebrate Morphology, Washington DC.

Wall CE, Vinyard CJ, Johnson KR, Williams SH, Hylander WL. 2006. Phase II jaw movements and masseter muscle activity during chewing in *Papio anubis*. Am J Phys Anthropol 129:215–224.

Wiersma JH. 2001. Maximum estimated bite force, skull morphology, and primary prey size in North American carnivores. MSc Thesis, Laurentian University (Ontario).

Wilson DE, Mittermeier R. 2009. *Handbook of the mammals of the world. Vol. 1. Carnivores*. Barcelona: Lynx Edicions.

Zabala J, Zuberogoitia I. 2003. Badger, *Meles meles* (Mustelidae, Carnivora), diet assessed through scat-analysis: a comparison and critique of different methods. Folia Zool 52:23–30.

Zhou YB, Newman C, Xu WT, Buesching CD, Zalewski A, Kaneko Y, Macdonald DW, Xie ZQ. 2011. Biogeographical variation in the diet of Holarctic martens (genus Martes, Mammalia: Carnivora: Mustelidae): adaptive foraging in generalists. J Biogeogr 38:137–147.